HAL open science

Modeling convective drying of food products: the case study of yacon (Smallanthus sonchifolius)

Bianca Cristine Marques, Artemio Plana-Fattori, Carmen Cecilia Tadini, D. Flick

To cite this version:

Bianca Cristine Marques, Artemio Plana-Fattori, Carmen Cecilia Tadini, D. Flick. Modeling convective drying of food products: the case study of yacon (Smallanthus sonchifolius). 12th International Conference on Simulation and Modelling in the Food and Bio-Industry (FOODSIM'2022), Apr 2022, Gand, Belgium. hal-03634455

HAL Id: hal-03634455

https://hal.science/hal-03634455v1

Submitted on 7 Apr 2022

HAL is a multi-disciplinary open access archive for the deposit and dissemination of scientific research documents, whether they are published or not. The documents may come from teaching and research institutions in France or abroad, or from public or private research centers.

L'archive ouverte pluridisciplinaire **HAL**, est destinée au dépôt et à la diffusion de documents scientifiques de niveau recherche, publiés ou non, émanant des établissements d'enseignement et de recherche français ou étrangers, des laboratoires publics ou privés.

MODELING CONVECTIVE DRYING OF FOOD PRODUCTS: THE CASE STUDY OF YACON (*Smallanthus sonchifolius*)

Bianca Cristine Marques ([1,2]), Artemio Plana-Fattori ([3])([#]), Carmen Cecilia Tadini ([1,2]), and Denis Flick ([3])

([1]) Universidade de São Paulo, Escola Politécnica, Chemical Engineering Department,
Main *Campus*, Butantã, 05508-010 São Paulo, SP, Brazil
([2]) Universidade de São Paulo, FoRC/NAPAN Food Research Center
([3]) Université Paris-Saclay, INRAE, AgroParisTech, UMR SayFood, 91300 Massy, France
([#]) author corresponding address: AgroParisTech, Dept. MMIP, 16 rue Claude Bernard, 75231 Paris
E-mail: artemio.planafattori@agroparistech.fr

KEYWORDS

convective drying, shrinkage, yacón, diffusivity coefficient

ABSTRACT

The convective drying of a food product whose dehydration occurs under large deformation is studied. A numerical model is proposed for solving the heat and water mass transfer phenomena for cylindrical samples while including shrinkage. It is assumed that no porosity appears during drying. The finite volume method is applied, and mesh boundaries move with the dry matter. No information about the product's mechanical properties is required; shrinkage is predicted from geometrical considerations only. The approach is illustrated for the case of yacón samples, whose reduction in volume can reach 90 % after a few hours of drying. Previous work with a convective dryer pilot unit under controlled air temperature and relative humidity is considered, firstly in identifying key parameters related to the volume reduction and to the water diffusivity in the product, secondly in assessing the drying kinetics as predicted by the model.

INTRODUCTION

The shrinkage of fruits and vegetables strongly depends on their mechanical properties. The development of shrinkage models has assumed fruits and vegetables as elastic, hyperelastic, elasto-plastic or visco-elastic. Their heterogeneous structure turns very complex the actual shrinkage behavior. For instance, most of the available literature considered the modulus of elasticity of potato tissue as a function of water content, based on data from experiments conducted at room temperature (e.g. Yang *et al.*, 2001); however, the modulus of elasticity depends on the temperature and the material structure. The correlation developed for potato may not be applicable for other food materials due to their diverse nature and properties. For a realistic understanding, an accurate relationship of modulus of elasticity could be based on data generated while drying is in progress (Mahiuddin *et al.*, 2018). The assessment of thermo-physical and mechanical properties of food materials as a function of temperature and water content along the drying process certainly constitutes an interesting research topic. Looking for model development and given the wide variety of food materials, it would be desirable if alternatives exist to such a challenge.

Here we pursue the development of an approach for studying the evolution of food products that can experience significant shrinkage under convective drying. The original contribution lies in the experimental-based geometrical considerations for estimating how shrinkage is distributed in different directions. The detailed mechanical behavior of the food material is not required. The approach is implemented in a flexible numerical model which includes i) the coupling between heat and water mass transfer, and ii) the variation of water diffusivity in the food matrix with the moisture itself. These features have been quoted as mandatory in modeling moisture profiles during the drying process (Perré, 2015).

The approach is illustrated for cylindrical slices of yacón (*Smallantus sonchifolius*), a plant cultivated originally in the Andean region for its tuberous, mildly sweet roots. The interest in yacón has increased (Caetano *et al.*, 2016): it constitutes a good option for low- carbohydrate diets because of its low amounts of sucrose and glucose, and its high amount of non-digestible carbohydrates. The industrial utilization of yacón is quite broad (Lebeda *et al.*, 2012). More than 70 % of the fresh tuberous root biomass of yacón is composed of water (Lachman *et al.*, 2003). Water activity is high, leading to a short shelf-life; partial hydrolysis of oligo-fructans can start a few days after harvest (Graefe *et al.*, 2004). Drying is a convenient way to prepare yacón for storage, and the influence of drying conditions on its composition has been investigated (Scher *et al.*, 2009; Campos *et al.*, 2016; Khajehei *et al.*, 2018a; Salinas *et al.*, 2018). Shrinkage cannot be neglected in studying the evolution of yacón submitted to convective drying: the sample shape can be completely changed and the reduction in volume can reach 90 % (Bernstein and Norena, 2014). The evolution of yacón slices under convective drying constitutes an interesting case study for discussing the possibilities and the limitations of an approach for estimating shrinkage without information about the product's mechanical properties.

The numerical model proposed in the pioneering work of Marques *et al.* (2020a) is here improved, mainly by expressing the diffusivity of water in yacón as a function of local temperature and water content values in the food matrix. Attention is focused on one of the air convective drying conditions studied experimentally by Marques *et al.* (2020b).

PHYSICAL MODEL

The convective drying of a slice of food matrix is hereafter studied by taking into account the following assumptions:

- evaporation occurs at the surface only;
- energy transfer occurs due to heat conduction inside the food matrix and water convection at its surface;
- liquid water migrates inside the product relatively to dry matter following moisture gradient; and
- no porosity appears during drying.

The last assumption means that, locally, the total volume occupied by the food matrix containing 1 kg of dry matter can be expressed as the sum of volumes that are occupied by dry matter and water:

$$\frac{1}{\rho_{dm}} = \frac{1}{\rho^{\#}_{dm}} + \frac{X_w}{\rho^{\#}_{w}} \tag{1}$$

wherein ρ_{dm} is expressed in kg of dry matter [kg-dm] by cubic meter of food product; X_w is the water content in the food product, dry basis [kg-w/kg-dm]; and $\rho^{\#}_{dm}$ and $\rho^{\#}_{w}$ are the dry matter and water mass densities [kg/m^3] (see Table).

The conservation equation for the water content can be expressed, in its convective form, as:

$$\frac{\partial X_w}{\partial t} + \vec{v}_{dm} \cdot \vec{\nabla} X_w = \frac{1}{\rho_{dm}} \vec{\nabla} \cdot \vec{j}_{w/dm} \tag{2}$$

wherein $\vec{v}_{dm}$ is the dry matter velocity in the food slice. The water flux relative to the dry matter is given by:

$$\vec{j}_{w/dm} = -D_w \vec{\nabla} (\rho_{dm} X_w) \tag{3}$$

wherein D_w is the water diffusivity [m^2/s] in the food product. Equation 2 is solved by taking into account the following boundary condition at the food matrix surfaces:

$$\vec{j}_{w/dm} \cdot \vec{n} = k \left(a_w\{X_w\} C_{sat}\{T\} - RH_{air} C_{sat}\{T_{air}\} \right) \tag{4}$$

wherein k is the mass transfer coefficient [m/s], $a_w\{X_w\}$ is the water activity in the product at the water content X_w, and $C_{sat}\{T\}$ is the saturated water vapor concentration at the temperature T [kg-w/m^3].

The internal energy of the food product (by kg of dry matter) is the sum of the internal energies of dry matter and water:

$$u = u_{dm} + X_w u_w = \left(C^{\#}_{dm} + X_w C^{\#}_{w} \right) T \tag{5}$$

wherein $C^{\#}_{dm}$ and $C^{\#}_{w}$ are the dry matter and water heat capacities [J/kg-dm/K]. The conservation equation for the internal energy can be expressed as:

$$\frac{\partial u}{\partial t} + \vec{v}_{dm} \cdot \vec{\nabla} u = \frac{1}{\rho_{dm}} \left(\vec{\nabla} \cdot \vec{j}_{w/dm} u_w + \vec{\nabla} \cdot \vec{j}_q \right) \tag{6}$$

wherein the energy flux is given by:

$$\vec{j}_q = -\lambda \vec{\nabla} T \tag{7}$$

wherein λ is the bulk thermal conductivity, obtained as $\lambda = (\lambda^{\#}_{dm})^{\alpha} (\lambda^{\#}_{w})^{(1-\alpha)}$; $\lambda^{\#}_{dm}$ and $\lambda^{\#}_{w}$ are the dry matter and water thermal conductivities [W/m/K], and α is the volume fraction occupied by dry matter in the food matrix. Equation 6 is solved by taking into account the following boundary condition at the food matrix surfaces:

$$\vec{j}_q \cdot \vec{n} = h \left(T - T_{air} \right) + L_v \vec{j}_{w/dm} \cdot \vec{n} \tag{8}$$

wherein h is the heat transfer coefficient [W/m^2/K] and L_v is latent heat of water vaporization [J/kg].

Water diffusivity in the product is required for evaluating water migration inside the food matrix (equation 3). The two phase model proposed by Maroulis *et al.* (2001) is used:

$$D_w\{X_w, T\} = \frac{1}{1+X_w} D_{w,dry}\{T\} + \frac{X_w}{1+X_w} D_{w,wet}\{T\} \tag{9}$$

$$D_{w,dry}\{T\} = D_{dry} \exp\left(-\frac{E_{dry}}{R} \left(\frac{1}{T} - \frac{1}{T_{ref}} \right) \right) \tag{10}$$

$$D_{w,wet}\{T\} = D_{wet} \exp\left(-\frac{E_{wet}}{R} \left(\frac{1}{T} - \frac{1}{T_{ref}} \right) \right) . \tag{11}$$

Activation energy values for diffusion in dry (E_{dry}) and wet material (E_{wet}) were both assumed to be 30 kJ/mol, from experimental convective drying of yacón (Shi *et al.*, 2013). Reference temperature T_{ref} was chosen 60 °C. Diffusivity values in dry material (D_{dry}) and in wet material (D_{wet}) were identified by comparing observations and model predictions of dimensionless water content ($X^{\star}_w = X_w / X_{w,0}$).
Water activity in the product is required for evaluating surface evaporation. The Guggenheim-Anderson-deBoer isotherm equation was applied, and the parameters were estimated from desorption measurements of yacón samples at the reference temperature of 60 °C (Marques *et al.*, 2020b).

The crux of our approach is the representation of shrinkage, as a consequence of evaporation at the surface and water migration within the food matrix. Let us subdivide the food matrix before drying into a regular grid constituted by a large number of small volumes (cells). The development of porosity is neglected; hence moisture reduction is translated into water volume reduction and hence into total volume reduction at a local scale. Because the mass of dry matter contained in each cell remains constant, there is a displacement of dry matter along the drying. The velocity of this displacement corresponds to the vector $\vec{v}_{dm}$ in equations 2 and 6.

The blue line in Fig. 1 evidences that the diameter reduction of yacón slices under drying does not follow an isotropic shrinkage behavior, which corresponds to $\beta = 1/3$. Looking for a better match with experimental results, we focused the attention on the values of slice diameter and volume under vanishing water content. On one hand, Fig. 1 suggests $D^\star \sim 0.6$ for the fully dried matrix. On the other hand, the application of equation 1 to $X_w \to 0$ and then to $X_w = X_{w,0}$ provides $V^\star \sim 0.05$. Combining these results we reach a value close to $\beta = 1/6$, which is considered in the calculation of diameter reduction in the numerical model.

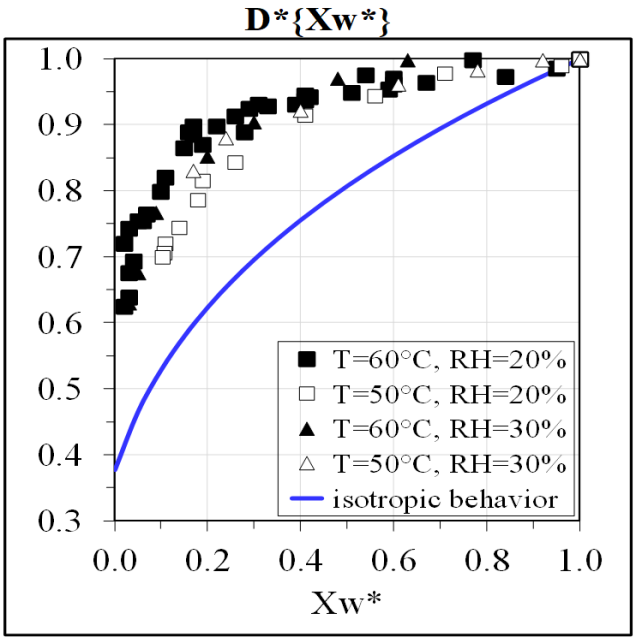

Figure 1: Dimensionless diameter of yacón slices, as a function of dimensionless water content: observations under selected convective drying conditions reported by Marques *et al.* (2020b) and predictions based upon isotropic shrinkage.

NUMERICAL MODEL

In the beginning, the food matrix is assumed to have a cylindrical shape with radius R_0 and height H_0. The matrix is assumed to be steadily exposed to a uniform transfer of heat and mass across all its surfaces, suggesting the adoption of the same value for the heat transfer coefficients at the upper, lower and lateral surfaces.

The food matrix is represented by a two-dimensional (2D) axis-symmetrical computational domain with radius R_0 and height $Z_0 = H_0/2$. The lower boundary of the domain corresponds to the plane of symmetry which divides the matrix into two identical halves. The finite volume method is applied, and the domain is subdivided into a number of control volumes (cells).

When drying starts ($t = 0$) all the cells are rectangular. In the present study, the mesh is built considering I and J cells along the radial and the axial directions; coordinates have the origin at the slice center. The computational domain has an initial aspect ratio $R_0/Z_0 \sim 6$; meshes are chosen in taking $I = 6 * J$. The (i,j)-th cell is characterized by:

- a bulk position $[r(i,j),\ z(i,j)]$, required in the evaluation of energy and water mass rates; the position of inner cells is defined as their center, the position of the outer cells is defined at the surface of the domain;
- four vertices; $[R(i,j), Z(i,j)]$ at its left-bottom corner;
- the surface $\Delta S(i,j) = \pi(R(i+1,j)^2 - R(i,j)^2)$ between two successive radial distances;
- the height $\Delta Z(i,j) = Z(i,j+1) - Z(i,j)$; and
- the width $\Delta R(i,j) = R(i+1,j) - R(i,j)$.

During the drying period ($t > 0$), the food matrix is submitted to convective heating and evaporation at its surface and to heat conduction and water migration inside. Independently on the drying state of the food matrix, all the cells are assumed to be trapezoids, the vertical sides of which are imposed to be parallel to the axis of symmetry. Their shape can be distorted as a consequence of distinct heat and mass transfer phenomena along with the axial and radial directions.

Each cell is associated with a single value for the product temperature and for the water content. In the beginning, initial values T_0 and $X_{w,0}$ are assigned to all the cells. Once the initial volume V_0 of each cell is known, it is possible to calculate the mass of dry matter m_{dm} contained therein:

$$m_{dm} \;=\; \rho_{dm,0}\, V_0 \tag{12}$$

wherein the initial density of dry matter in the food matrix can be expressed from equation 1. The mass of dry matter contained in each cell remains constant along with drying.

Convective conditions are assumed to be steady and defined by the air temperature (T_{air}) and relative humidity (RH_{air}). Such a situation causes heat and water mass exchanges between the product and the ambient air along the drying. After a time step (Δt), the total variation in the water content in the (i,j)-th cell and that in the temperature associated with this cell are calculated as :

$$\begin{aligned}\Delta X_w(i,j) \;=\; &(\,(\,(\phi_Z(i,j) - \phi_Z(i,j{+}1)) + \\ &+\ (\phi_R(i,j) - \phi_R(i{+}1,j)\,)\,)\,\Delta t/m_{dm}(i,j)\end{aligned} \tag{13}$$

$$\begin{aligned}\Delta T(i,j) \;=\; &(\,(\,(\Phi_Z(i,j) - \Phi_Z(i,j{+}1)) + \\ &+\ (\Phi_R(i,j) - \Phi_R(i{+}1,j)\,)\,)\,\Delta t/(m_{dm}(i,j)\, C_P(i,j))\end{aligned} \tag{14}$$

wherein $C_P = C^{\#}_{dm} + X_w C^{\#}_w$. These equations employ rates of change (i.e. variations per unit of time) of the water mass (ϕ [kg-w/s]) and of the internal energy (Φ [J/s]) along the axial Z- and radial R- directions. In the case of inner cells, the

water and energy rates are calculated as:

$$\phi_Z(i,j) = \Delta S(i,j)\, D_w(i,j)\, \rho_{dm}(i,j) \times (X_w(i,j-1) - X_w(i,j))/(z(i,j) - z(i,j-1)) \quad (15)$$

$$\phi_R(i,j) = 2\,\pi\, \Delta Z(i,j)\, D_w(i,j)\, \rho_{dm}(i,j) \times (X_w(i-1,j) - X_w(i,j))/(\ln(r(i,j)/r(i-1,j))) \quad (16)$$

$$\Phi_Z(i,j) = \Delta S(i,j)\, \lambda(i,j) \times (T(i,j-1) - T(i,j))/(z(i,j) - z(i,j-1)) \quad (17)$$

$$\Phi_R(i,j) = 2\,\pi\, \Delta Z(i,j)\, \lambda(i,j) \times (T(i-1,j) - T(i,j))/(\ln(r(i,j)/r(i-1,j))) \,. \quad (18)$$

Water and energy rates are calculated at surface cells while respecting the boundary conditions of the problem (equations 4 and 8). For instance, in the case of the lateral surface:

$$\phi_R(I+1,j) = 2\,\pi\, r(I,j)\, \Delta Z(I+1,j) \times k \times (a_w(I,j)\, C_{w,sat}\{T(I,j)\} - RH_{air}\, C_{w,sat}\{T_{air}\}) \quad (19)$$

$$\Phi_R(I+1,j) = 2\,\pi\, r(I,j)\, \Delta Z(I+1,j) \times h \times (T(I,j) - T_{air}) + L_v\, \phi_R(I+1,j) \,. \quad (20)$$

Thus, energy rates at the surface are computed by adding two contributions: the first is proportional to the difference between the temperature in the product and in the ambient air, the second is proportional to the water mass rate.

After updating temperature and moisture values (equations 13-14), the cell volume can be obtained (equation 1). Basic geometrical considerations are successively applied for recomputing the radial and vertical coordinates of cells' corners. Radial coordinates decreased with moisture reduction, following the $D^\star = (V^\star)^\beta$ relationship which was justified above; vertical coordinates are updated in a way to restore the cell volume.
During the drying, the cells at the axis of symmetry remained rectangular. The cell located at the axis of symmetry and at the plane of symmetry is the one associated with the slowest drying rate; its radial and vertical coordinates are the first to be updated.
The shape of the remaining cells is nearly unconstrained during the drying period: the only assumption is that their vertical sides remain parallel to the axis of symmetry.
The cells at the plane of symmetry are the longest in the slice; evaporation takes place only at the outer one only.
Cells that are located at the upper and lateral surfaces are strongly affected by evaporation and they quickly became very thin; such a finding seems realistic, because the moisture gradients therein are the highest. The representation of these phenomena guided us in building a mesh with a relatively narrower surface cells, comparatively with the inner cells (see Figure 4).

The algorithm was written in Python language, and there is no reason why it cannot be done with other computational means. No attempts were conducted in optimizing the algorithm.

Table: Key parameters considered in simulations.

air temperature	$T_{air} = 60$ °C (i)
air relative humidity	$RH_{air} = 20$ % (i)
slice initial temperature	$T_0 = 20$ °C (i)
slice initial water content	$X_{w,0} = 11$ kg-w/kg-dm (i)
slice initial height	$Z_0 = 0.007$ m (i)
slice initial radius	$R_0 = 0.02$ m (i)
water density	$\rho_w^\# = 991$ kg/m^3 (ii)
water heat capacity	$C_w^\# = 4180$ J/kg/K (ii)
water thermal conductivity	$\lambda_w^\# = 0.631$ W/m/K (ii)
dry matter density	$\rho_{dm}^\# = 1590$ kg/m^3 (iii)
dry matter heat capacity	$C_{dm}^\# = 1620$ J/kg/K (iii)
dry matter th. conductivity	$\lambda_{dm}^\# = 0.250$ W/m/K (iii)
latent heat of vaporization	$L_v = 2.36\ 10^6$ J/kg (iv)
heat transfer coefficient	$h = 32$ W/m^2/K (v)
mass / heat transfer coeff.	$k/h = 1.02\ 10^{-3}$ (vi)
mesh	$J = 5$ (vii)
	$I = 6 \times J = 30$ (vii)
time step	$\Delta t = 0.01$ s (vii)

(i) Drying convective conditions (Marques *et al.*, 2020b).
(ii) Values at 40 °C (average between the slice initial temperature and the air temperature).
(iii) Data provided by Hermann *et al.* (1999) about nine accessions of fresh yacón allowed us to estimate the averaged composition: 0.37g/100g for proteins, 0.024g/100g for fat, 11g/100g for carbohydrates, 0.36g/100g for fibers, and 0.51g/100g for ash. These values were considered in applying Choi and Oikos' (1986) approach for estimating yacón thermal properties at the temperature of 40 °C.
(iv) Value at 60 °C (air temperature).
(v) Value estimated after assuming that all the incoming heating is consumed into surface evaporation at the wet-bulb temperature. Such an estimation required the drying rate $dX_w^\star/dt$, whose value $1.4\ 10^{-4}$ s^{-1} at $t = 0$ was obtained by fitting experimental measurements of water content $X_w^\star$ during the drying.
(vi) According to the mass-heat transfer analogy, the ratio of mass to heat transfer coefficients can be expressed by using the Lewis number, as $Le^{-2/3}/(\rho\, C_P)$. Lewis number ~ 0.90 assuming air thermophysical properties at T_{air}.
(vii) Compromise between the reliability of model predictions and the computational cost (typically, 3 hours on a 11 Gen Intel Core i7-1165G7 at 2.8 GHz, 16 Gb-RAM laptop).

RESULTS AND DISCUSSION

At this step of development of the model, only the drying conditions [air flow 4 m/s, T_{air} = 60 °C, RH_{air} = 20 %] are taken into account. These were the most reproducible among the experimental tests conducted by Marques *et al.* (2020b) in drying yacón samples with a pilot unit convective dryer.

Figure 2A displays measurements of water content conducted under these conditions, as described by Marques *et al.* (2020b). The black line indicates model predictions reached after assuming, in equation 10, the values $D_{dry} = 4.4\ 10^{-12}$ m^2/s and $D_{wet} = 1.7\ 10^{-10}$ m^2/s for water diffusivity in dry and wet material, respectively. The root-mean-square error was about 0.023 in $X_w^\star$ units. The vanishing value of water diffusivity under dry conditions is consistent with the product structure, nearly crumbly / brittle, after six hours of drying.
Figure 2C presents the total surface reduction along the drying. A first decreasing tendency can be recognized from the beginning down to $X_w^\star \sim 0.4$ when the diameter reduction becomes progressively more significant (Figure 3C); later on, the total surface decreases to 30-35 % of its initial value.
Figures 2B and 2D show the dimensionless drying kinetics $dX_w^\star/dt$ and $dX_w^\star/dt.S^\star$. Both derivatives should be directly proportional to $X_w^\star$ according to Lewis' (1921) drying approach. That classical model assumes no shrinkage along the drying, which is unsuitable for yacón samples. Model predictions indicate a more complex behavior for $dX_w^\star/dt$; actually, this derivative includes the decreasing tendencies at the surface and the core, which can be different and unsteady along the process (see below). Figures 2E and 2F compare model predictions with the measurements of dimensions of yacón slices as obtained by Marques *et al.* (2020b) under the same drying conditions. Model results and observations of the slice height are hard to compare: on one hand, predictions of height correspond to the axis of symmetry; on the other hand, the upper and lower surfaces of the samples become rough along the drying, reducing the accuracy of the thickness measurement. The general decreasing tendencies of slice height and diameter are captured by model predictions.

In addition to bulk results about the food matrix under drying, the approach allows studying the evolution of elementary volumes therein. Figure 3 presents selected properties at two opposite positions along the axis of symmetry of the food slice: at the surface (1) and the core (2). Position 1 moves along with the shrinkage history, being always located at the slice surface; it is exposed to moisture gradients that are stronger than that at position 2.
Figure 3A reveals that these positions follow almost the same temperature history; such a finding comes from a combination of the small distance separating these positions and high thermal conductivity in the product (see below). Beginning at $T_0 = 20$ °C, the temperature quickly reaches the wet-bulb temperature (about 34 °C), allowing favorable conditions to evaporation at the surface.

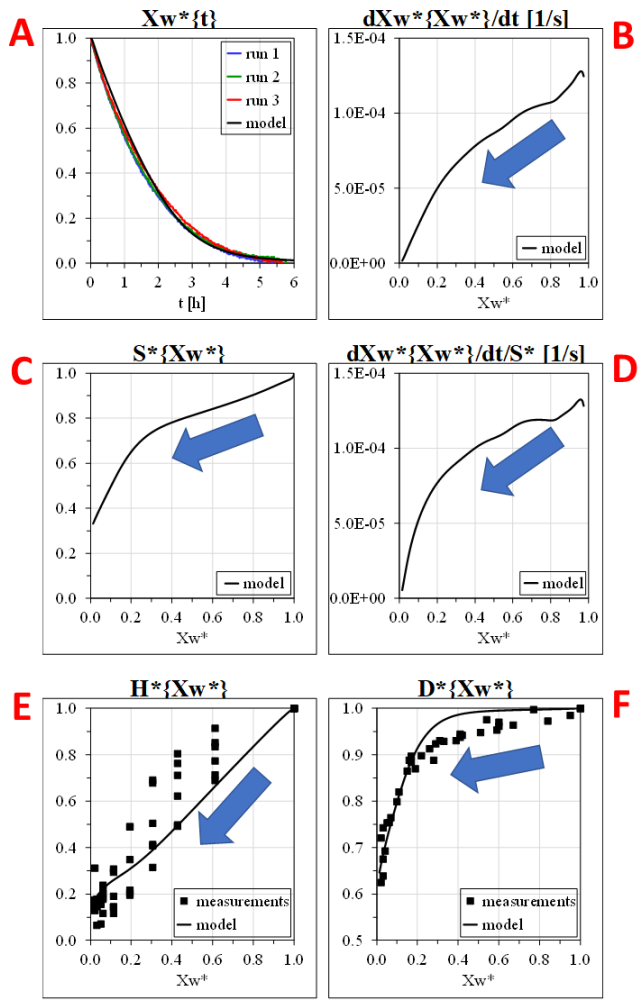

Figure 2: State of the food slice according to model predictions (black lines) and to observations of mass loss (colored lines) and of slice dimensions (squares), under drying conditions [air flow 4 m/s, T_{air} = 60 °C, RH_{air} = 20 %]. Arrows recall that water content decreases along the drying.

Figure 3B presents the water content history at these positions. Convective drying is effective: after 1.5 h, it remains about 2 % of the initial water content at the surface. At this time, drying really starts at the core, following a slow-fast-slow decreasing tendency. After six hours of drying there remains about 4 % of the initial water content at the core.
Water diffusivity in the product is assumed to depend on both temperature and moisture, whose relative importance evolves as heating and drying progress with time. The influence of temperature decreases as the product reaches $T_{ref} = 60$ °C (equations 10 and 11). The influence of moisture is more complicated: our results indicate that the water diffusivity value in wet material is more than 30 times superior in dry material (see above) and, as expected, their relative importance depends on the water mass fraction.

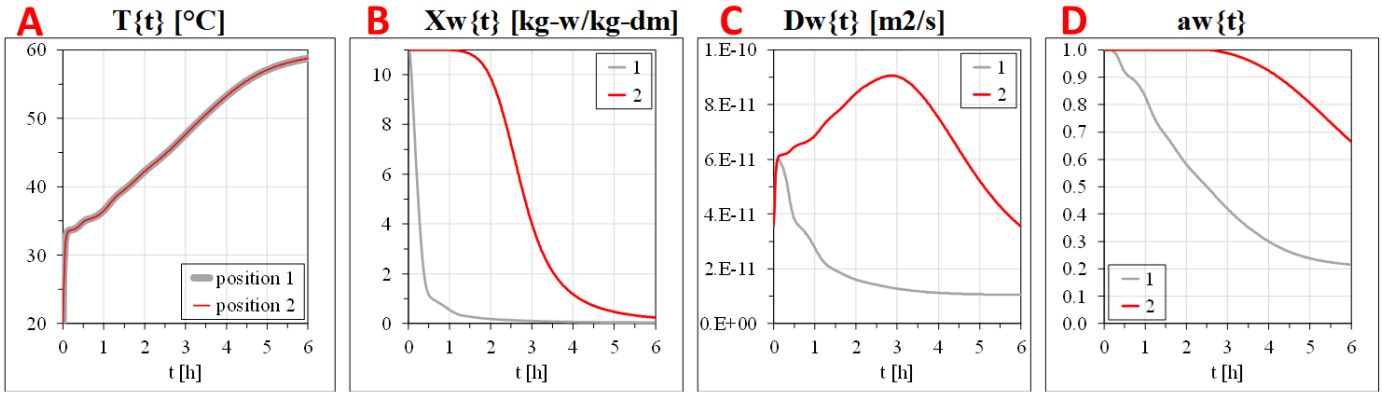

Figure 3: Selected properties in two positions along the axis of symmetry of the food slice: at the surface (1) and at the core (2).

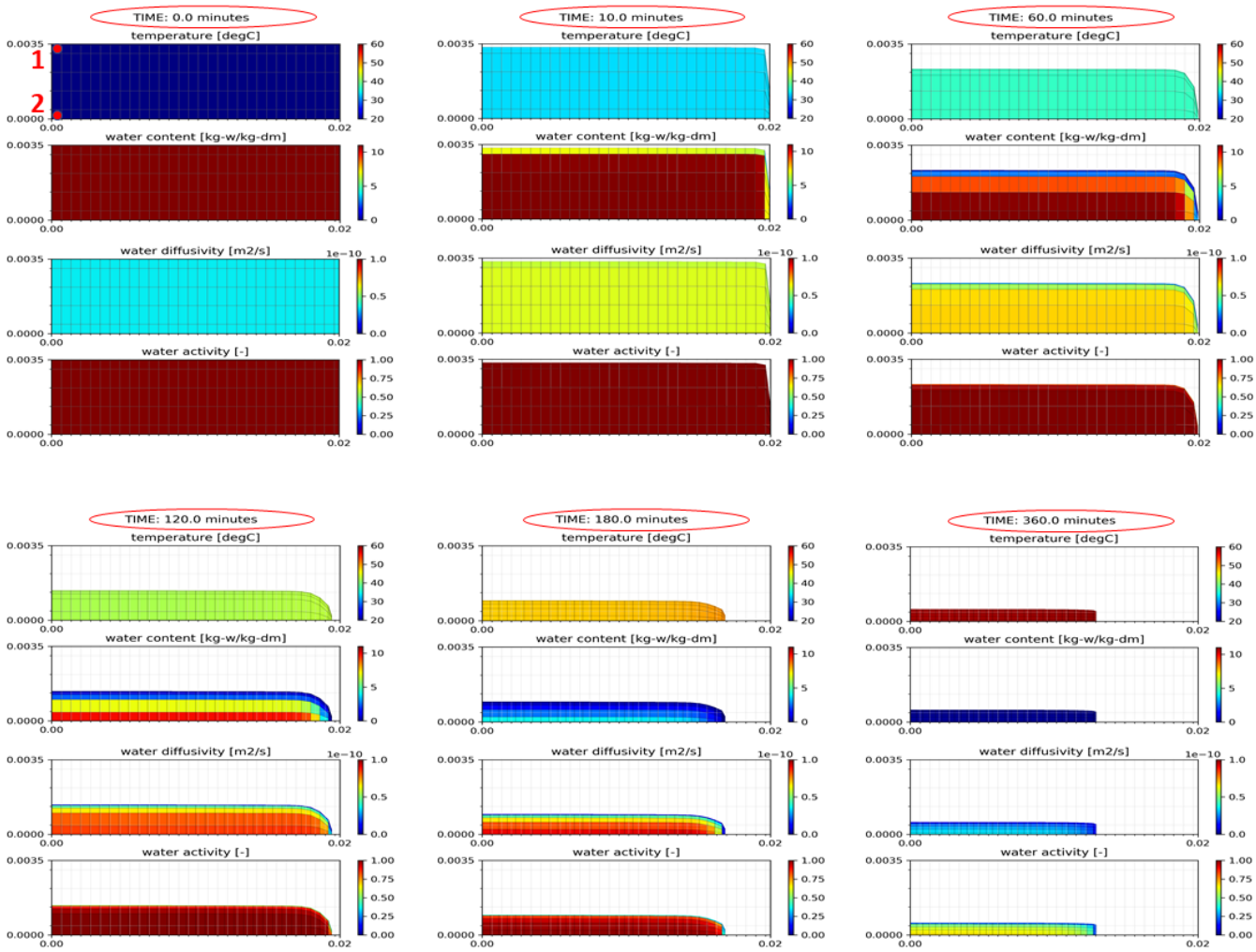

Figure 4: Temperature, water content, water diffusivity and water activity fields in the food slice at selected times. Dimensions of the food slice are expressed in meters. Positions 1 and 2 considered in Figure 3 are also displayed.

Figure 3C shows that, at the surface, water diffusivity decreases from 6 10^{-11} to 10^{-11} m^2/s along the drying. In other words, even after six hours of drying, the 'wet material' component of equation 9 still plays a non-negligible role. At the core, the water diffusivity follows an increasing tendency until drying effectively starts therein (after about three hours of drying); later on, the influence of moisture reduction becomes dominant.
The evolution of water activity (Figure 3D) is delayed with respect to that of water activity and that of water content (Figure 3B). This result comes from high activity values even under moderate moisture values (e.g. $a_w \sim 0.99$ at $X_w \sim 4.5$ kg-w/kg-dm). Figure 3D highlights that the water activity is not homogeneous across the product slice, even after six hours of convective drying.

Previous figures have shown properties of the food matrix, both for the entire slice (Figure 2) and at positions that seem opposite (Figure 3), during whole the drying. Figure 4 provides a third perspective, displaying the temperature, water content, water diffusivity and water activity fields throughout the food slice at selected times.

I... A remarkable result is the thermal homogeneity of the product slice, during the whole drying period. An explanation is provided by the low values of Biot number $h(H/2)/\lambda$; its decreasing tendency (0.2 down to 0.06) is due to a stronger decrease in height (0.007 down to 0.001 m) than in thermal conductivity (0.6 down to 0.3 W/m/K).

II... As expected, evaporation at the surface drives the water migration across the food slice. The lateral surface of the slice experiences faster drying than its upper and lower surfaces. After six hours under the convective drying conditions here considered, the slice volume decreased to about 7 % of its initial value.

III... Water diffusivity varies with time and space following a complex pattern. At the slice surface, its decreasing tendency is driven by the moisture reduction; such a tendency is also verified in the whole slice after about three hours when drying effectively starts at the core (see Figure 4C). The influence of temperature decreases along the drying period, as the slice achieves the reference temperature 60 °C.

IV... Water activity remained high after four hours, over 0.90 throughout large portions of the product slice, suggesting favorable conditions to selected pathogens. Results indicate the importance of latest hours of drying in effectively reducing the water activity at the slice core.

All these remarks apply after employing finer and coarser meshes in solving the same problem (results not shown). The time and spatial distributions displayed in Figure 4 put in evidence the strong coupling between heat and water mass transfer phenomena during the convective drying of a food slice.

Lastly, to the authors' knowledge, these results represent the first efforts in displaying how the water diffusivity and water activity evolve throughout a food matrix exposed to convective drying.

CONCLUSIONS AND RECOMMENDATIONS

We demonstrate that selected properties of a food slice under convective drying can be studied with a simple model including shrinkage. Our approach assumes that the volume reduction is primarily driven by the diameter reduction, i.e., by decreasing moisture at the plane of symmetry of the product slice. The assessment of such a tendency was possible from measurements of slice diameter.
In this study, the water diffusivity in yacón samples was approximated through the two-phase structural model proposed by Maroulis *et al.* (2001). Water diffusivity values under dry and wet conditions were identified after comparing the evolution of moisture from the experiment and model. These values are about 100 and 10 times smaller than similar associated with potato in the literature.
Future work should assess the reliability of this approach under other convective drying conditions, while conducting additional efforts in identifying the parameters required by the two phase model. Testing this approach should consider wider ranges of ambient conditions (air flow, temperature and relative humidity) and including different varieties of yacón and later other raw food products. Much work remains to be done in order to clarify the relationship between shrinkage and moisture loss.

ACKNOWLEDGEMENTS

Authors B.C.M. and C.C.T. received grants from Brazilian agencies: grants 2018 / 21327-1, 2019 / 21832-0, and 2013 / 07914-8 from the São Paulo Research Foundation (FAPESP); finance code 001 from the Coordination for the Improvement of Higher Education Personnel (CAPES); and grant 306414 / 2017-1 from the National Council for Scientific and Technological Development (CNPq). We warmly acknowledge AgroParistech and UMR SayFood for kindly receiving the first named author for a one-year research internship.

REFERENCES

Bernstein, A.; and Norena, C. P. Z. 2014. "Study of thermodynamic, structural, and quality properties of yacón (*Smallanthus sonchifolius*) during drying". *Food and Bioprocess Technology*, 7, 148-160.

Caetano, B. F. R.; Moura, N. A.; Almeida, A. P. S., Dias; M. C., Sivieri, K.; and Barbisan, L. F. 2016. "Yacón (*Smallanthus sonchifolius*) as a food supplement: Health-promoting benefits of frutooligosaccharides". *Nutrients*, 8, 436.

Campos, D.; Aguilar-Galvez, A.; and Pedreschi, R. 2016. "Stability of fructooligosaccharides, sugars and colour

of yacón (*Smallanthus sonchifolius*) roots during blanching and drying". *International Journal of Food Science and Technology*, 51, 1177-1185.

Choi, Y.; and Okos, M. R. 1986. "Effects of temperature and composition on the thermal properties of foods". In M. Le Mageur, P. Jelen (Eds.), *Food Engineering and Process Applications* (pp. 93-101). Elsevier Applied Science.

Graefe, S.; Hermann, M.; Manrique, I.; Golombek, S.; and Buerkert, A. 2004. "Effects of post-harvest treatments on the carbohydrate composition of yacón roots in the Peruvian Andes". *Field Crops Research*, 86, 157–165.

Hermann, M.; Freire, I.; and Pazos, C. 1999. "Compositional diversity of the yacón storage root". In *Andean Roots and Tuber Crops* (pp. 425-432). International Potato Center Program Report 1997-1998.

Khajehei, F.; Hartung, J.; and Graeff-Hönninger, S. 2018. "Total phenolic content and antioxidant activity of yacón (*Smallanthus sonchifolius Poepp. and Endl.*) chips: Effect of cultivar, pre-treatment, and drying". *Agriculture*, 8, 183.

Lachman, J.; Fernández, E. C.; and Orsák, M. 2003. "Yacón [*Smallanthus sonchifolia (Poepp. et Endl.) H. Robinson*] chemical composition and use: A review". *Plant, Soil and Environment*, 49, 283–290.

Lebeda, A., Doležalová, I., Fernández, E.; and Viehmannová, I. 2012. Yacón (*Asteraceae; Smallanthus sonchifolius*). In R. J. Singh (Ed.), *Genetic Resources, Chromosome Engineering, and Crop Improvement*. Volume 6: Medicinal Plants (pp. 641-702). CRC Press.

Lewis, W. K. 1921. "The rate of drying the solid materials". *The Journal of Industrial and Engineering Chemistry*, 13, 427-432.

Mahiuddin, M.; Khan, M. I. H.; Kumar, C.; Rahman, M. M.; and Karim, M. A. 2018. "Shrinkage of food materials during drying: Current status and challenges". *Comprehensive Reviews in Food Science and Food Safety*, 17, 1113-1126.

Marques, B. C.; Plana-Fattori, A.; Tadini, C. C.; and Flick, D. 2020a. "Modeling convective drying of food products under large deformation". *Eleventh International Conference on Simulation and Modelling in the Food and Bio-Industry (FOODSIM'2020) (April 2020, Ghent, Belgium)*.

Marques, B. C.; Plana-Fattori, A.; and Tadini, C. C. 2020b. "Data acquisition for modelling convective drying of yacón (*Smallanthus sonchifolius*) slices". *Eleventh International Conference on Simulation and Modelling in the Food and Bio-Industry (FOODSIM'2020) (April 2020, Ghent, Belgium)*.

Maroulis, Z. B.; Saravacos, G. D.; Panagiotou, N. M.; and Krokida, M. K. 2001. "Moisture diffusivity data compilation for foodstuffs: Effect of material moisture content and temperature". *International Journal of Food Properties*, 4, 225-237.

Perré, P. 2015. "The proper use of mass diffusion equations in drying modeling: Introducing the drying intensity number". *Drying Technology*, 33, 1949-1962.

Salinas, J. G.; Alvarado, J. A.; Bergenstahl, B.; and Tornberg, E. 2018. "The influence of convection drying on the physico-chemical properties of yacón (*Smallanthus sonchifolius*)". *Heat and Mass Transfer*, 54, 2951-2961.

Scher, C. F.; Rios, A. O.; and Norena, C. P. Z. 2009. "Hot air drying of yacón (*Smallanthus sonchifolius*) and its effect on sugar concentrations". *International Journal of Food Science and Technology*, 44, 2169-2175.

Shi, Q.; Zheng, Y.; and Zhao, Y. 2013. "Mathematical modeling on thin-layer heat pump drying of yacón (*Smallanthus sonchifolius*) slices". *Energy Conversion and Management*, 71, 208-216.

Yang, H.; Sakai, N.; and Watanabe, M. 2001. "Drying model with non-isotropic shrinkage deformation undergoing simultaneous heat and mass transfer. *Drying Technology*, 19, 1441-1460.

BIOGRAPHIES

BIANCA CRISTINE MARQUES is a Brazilian Ph.D. student at the Univ. de São Paulo, being advised by Carmen. As a part of her research, she met Artemio and Denis during one year at AgroParisTech.

ARTEMIO PLANA-FATTORI studied Atmospheric Sciences at the Univ. de São Paulo and later in the Univ. Lille (Ph.D. in 1994). After 20 years teaching and doing research in Brazil, he joined AgroParisTech in 2010, where he works with numerical modeling applied to food engineering.

CARMEN CECILIA TADINI conducts research on food science and engineering, with applications in pasteurization, bakery, drying and biodegradable films by extrusion. She is Full Professor at the Univ. de São Paulo and author of one of the few textbooks about Food Engineering in Portuguese.

DENIS FLICK is Full Professor at AgroParisTech. He conducts research in modeling and numerical simulation of coupled phenomena in food processes (heat and mass transfer, fluid flow and product deformation, product transformation), with applications in food cold chain equipment, heat exchangers, cooking and baking, dairy products, bread, and ice cream. His teaching area includes transport phenomena, thermodynamics, and numerical modeling.